arXiv:hep-lat/0410050v1 28 Oct 2004

Hadron Spectrum from Dynamical Lattice QCD Simulations

K-I. Ishikawa[a]

[a]Department of Physics, Hiroshima University, Higashi-Hiroshima, Hiroshima 739-8526, Japan

Recent progress in unquenched lattice QCD simulations is reviewed with emphasis on understanding of chiral behavior for light quark masses.

1. Introduction

In the long standing challenge of the calculation of hadron spectrum from the first-principles lattice QCD simulation, the inclusion of dynamical quarks, or unquenching, has been the crucial but computationally demanding step. Thanks to the rapid increase of the computer power and recent developments in the lattice formulations and numerical algorithms, such simulations have become feasible in the past several years.

One of the stumbling block toward full QCD simulations has been the treatment of the third dynamical quark, *i.e.*, the strange quark. Since the standard HMC algorithm [1] assumes that the number of flavor is even, previous simulations including the odd number of flavors had to use a non-exact algorithm, such as the R algorithm [2], which contains a systematic error of order $\delta\tau^2$, with $\delta\tau$ the molecular dynamics step size. Recently an exact HMC algorithm with polynomial approximation has been developed [3] and this difficulty has been essentially removed.

A major problem in the dynamical fermion simulations is that the up and down quark masses are much smaller than the masses we can simulate on the lattice. Therefore, we usually extrapolate the data obtained at an order of magnitude larger sea quark masses to the physical point assuming some fitting ansatz. For the pseudo-scaler meson channel, the fitting ansatz can be justified by Chiral Perturbation Theory (ChPT), which provides a systematic expansion in terms of pion mass and momentum squared. However, the problem is that the region of applicability of ChPT is not known *a priori*, and the lattice data, for instance obtained by the JLQCD collaboration, do not indicate the non-analytic behavior expected from the next-to-leading order ChPT within simulated quark masses, *e.g.,* above $m_s/2$ for JLQCD [4].

Since the last year's Symposium, a number of unquenched lattice QCD simulations have been pursued to overcome the problems related to the chiral behavior of hadron spectrum, which I review in this talk. In Section 2 I summarize the major unquenched simulations available to date for both 2- and 2+1-flavor cases. In Section 3 I discuss the algorithmic issues and physics results from recent 2+1-flavor simulations. Discussion on the chiral extrapolation, which is the main focus of this review, is given in Section 4.

The theoretical background of the chiral perturbation theory is discussed by Bär[5,6] at this conference. For the unquenched calculations of quark masses, weak matrix elements, and heavy quark physics, see other reviews in [7,8,9].

2. Recent Unquenched QCD simulations

Table 1 summarizes the recent large-scale unquenched simulations with N_f dynamical flavors. The lattice spacing a, physical spatial extent of the lattice aL, and pseudo-scalar and vector meson masses M_{PS} and M_V at the unitary point (*i.e.,* valence quark mass equals sea quark mass) are listed.

Throughout this paper we use the following abbreviations to denote the lattice actions. The gauge and quark action combinations are denoted as, PW: plaquette gauge and unimproved Wilson quark actions, PC(X): plaquette gauge and clover quark actions with the improvement coefficient $c_{\rm SW}$ determined by a method X, RC(X): RG-improved gauge and clover quark actions with the

Table 1
Recent spectrum runs in dynamical QCD simulations. ([1] an update of [10,11], [2] an update of [12])

Collab.	N_f	Action	a [fm]	aL [fm]	M_π/M_ρ	M_π [GeV]	Ref.
MILC	2+1	SZAT	0.125, 0.09	2.5–3.0	0.58–0.30 0.49, 0.38	0.60–0.25	[13,14,15]
CP-PACS & JLQCD	2+1	RC(N)	0.1	1.6, 2.0	0.77–0.64	1.00–0.64	[16,17]
CP-PACS	2	RC(T)	0.22–0.09	2.6–2.1	0.8–0.5	1.2–0.5	[10,11]
CP-PACS	2	RC(T)	0.22	2.6	0.61–0.35	0.58–0.27	[18][1]
UKQCD	2	PC(N)	0.1	1.6	0.84–0.58	1.1–0.6	[12]
UKQCD	2	PC(N)	0.1	1.6	0.44	0.42	[19][2]
JLQCD	2	PC(N)	0.1	1.1–1.8	0.80–0.60	1.37–0.60	[20]
QCDSF & UKQCD	2	PC(N)	0.1	1.2–2.4	-	1.2–0.64	[21]
RBC	2	DBW2DW	0.12	1.9	-	0.49,0.61,0.70	[22]
qq+q	2	PW	0.20	3.2	-	0.66–0.37	[23,24]
SPQcdR	2	PW	0.066	1.1,1.6	0.6–0.8	-	[25]
GRAL	2	PW	0.13, 0.08	1.1–2.1	-	0.42–0.64	[26]
SESAM	2	PW	0.086	1.4	0.83–0.69	1.00–0.64	[27]
SESAM & TχL	2	PW	0.092, 0.076	1.3–1.8	0.83–0.57	0.90–0.49	[28,29]

improvement coefficient determined by a method X, SZAT : Symanzik improved gauge and AsqTad KS quark actions $O(a^2)$-improved at tree level, DBW2DW : DBW2 improved gauge and domain wall quark actions. The method X for clover quark action is either N: non-perturbatively determined, or T: tadpole estimated.

Let us touch upon the representative full QCD simulations. For the Wilson-type quark action, the continuum extrapolation was previously attempted by the CP-PACS collaboration [10,11] using data at three lattice spacings with $N_f = 2$ RC(T) action, and a better agreement of hadron masses than in the quenched case was observed in the continuum limit. Ref. [18] is an update of this work, which extends the simulation at the coarsest lattice spacing ($a \sim 0.22$ fm) toward smaller sea quark masses corresponding to $M_{\rm PS}/M_{\rm V}$ =0.60–0.35.

UKQCD [19] also recently extended their previous simulation [12] toward smaller quark masses. The SPQcdR collaboration reported their preliminary results for the light hadron spectrum, light quark masses and renormalization constants [25]. The GRAL collaboration [26] has started a study of the finite volume effect at small quark masses on small to medium-sized lattices. All these are $N_f = 2$ simulations.

The CP-PACS and JLQCD collaborations have jointly started $N_f = 2+1$ flavor simulations with the RC(N) action, and their first results for a $16^4 \times 32$ lattice appeared at the last lattice conference [16]. They have extend the physical volume to $20^3 \times 40$ this year.

The $N_f = 2$ and $2+1$ unquenched simulations with the KS-type fermions can be performed at smaller quark masses compared to the Wilson-type quark actions, because the required computational cost is much reduced. The 2+1-flavor simulations with the SZAT action have been carried out for several years by the MILC collaboration [13,14,15]. This year they reported a detailed analysis of the chiral and continuum extrapolations by adding data at smaller sea quark masses and finer lattice spacing.

With the configuration generated by the MILC collaboration, the "gold-plated" hadronic observables have been calculated by the HPQCD-MILC-UKQCD-Fermilab collaborations and good agreement with experimental results is observed [30].

The RBC collaboration reported the calculation of pseudo-scalar meson masses and decay constants using the unquenched domain wall fermion [31,22] for $N_f = 2$ case.

3. $N_f = 2 + 1$ simulations

3.1. Algorithmic issues

The simulation algorithm widely used for unquenched simulations is the Hybrid Monte Carlo algorithm [1]. Quarks are treated by the pseudo-fermion method [32], with which we can treat even number of them dynamically. If the single-flavor lattice Dirac operator D has a real positive determinant $\det[D]$, it is also possible to treat it as a probability distribution function for link variables. The naive application of the pseudo-fermion method to $\det[D]$ results in a complex effective action, however. This problem is avoidable by constructing an operator S which satisfies $S^2 = D$. The polynomial approximation and rational approximation can be used to construct such an operator [33]. With this method the HMC algorithm with the polynomial or rational approximated pseudo-fermion has been obtained. The algorithm is then combined with the usual two-flavor HMC algorithm to make an $N_f = 2+1$ flavor HMC algorithm [3]. The efficiency of the algorithm is comparable to that of the HMC algorithm [34].

For the KS-type quark actions, the fourth-root trick is widely used to express a single flavor of fermion. This amounts to taking a fourth-root of the determinant of the KS Dirac operator $D_{\rm KS}$, which represents four flavors of fermions in the continuum. This trick is combined with the R algorithm [2] for carrying out simulations.

An important issue with the R algorithm is controlling the systematic error of order $\delta\tau^2$ at finite molecular dynamics step size $\delta\tau$. It is argued that a condition $\delta\tau < m$ is needed [35] to avoid large systematic errors. A reliable estimate of the magnitude of error is difficult prior to the actual simulations.

In the MILC simulations [13,15] $\delta\tau \lesssim 3/2am$ is adopted with light dynamical quark mass am. The systematic error for some observables is investigated by comparing the results from additional simulations with larger $\delta\tau$. The additional runs are too short to conclude the $(\delta\tau)^2$ behavior for hadronic masses. Further investigation on this issue should be made by increasing the statistics or using exact algorithms as described below.

The polynomial approximation described for the Wilson-type quarks above can also be applied to $D_{\rm KS}^{1/4}$. This leads to the exact algorithms, the polynomial HMC which uses polynomial approximant and the rational HMC which uses rational approximant, have been developed for the two-flavor case [36,35,37,38]. For more details of the recent development of the simulation algorithm, see [39].

In order to justify the fourth-root trick one has to show the existence of a local fermion kernel D which satisfies $\det[D_{\rm KS}]^{1/4} = \det[D]$. Otherwise there is no guarantee that the continuum limit is real QCD. It is shown that a naive candidate $D = D_{\rm KS}^{1/4}$ is non-local [40,41], and the existence of a local operator D is still an open question. The related issues are discussed in [42,43,44].

3.2. $N_f = 2+1$ simulation with the Wilson-type fermions

The CP-PACS and JLQCD collaborations have started a joint program to perform realistic simulations including the dynamical strange quark. They performed simulations on two lattice volumes, $16^3\times32$ and $20^3\times40$, at a finite lattice spacing $a \sim 0.1$ fm with the RG-improved gauge action and non-perturbatively $O(a)$-improved Wilson action. In order to interpolate or extrapolate to the physical strange quark mass, the simulations are made at two strange quark masses corresponding to $M_{\rm PS,SS}/M_{\rm V,SS} \simeq 0.71$–$0.77$. For the light up and down quarks which are assumed degenerate, six (five) quark masses on the $16^3 \times 32$ ($20^3 \times 40$) lattice are simulated. It covers the range $M_{\rm PS,LL}/M_{\rm V,LL} \simeq 0.62$–$0.78$.

They calculated the light meson mass spectrum, and up and down, and strange quark masses. The meson masses are calculated at the unitary point where the valence and sea quarks have equal masses. Light and strange mesons are constructed with Light-Light (LL), Light-Strange (LS) and Strange-Strange (SS) combinations of simulated quarks. Chiral extrapolation is made

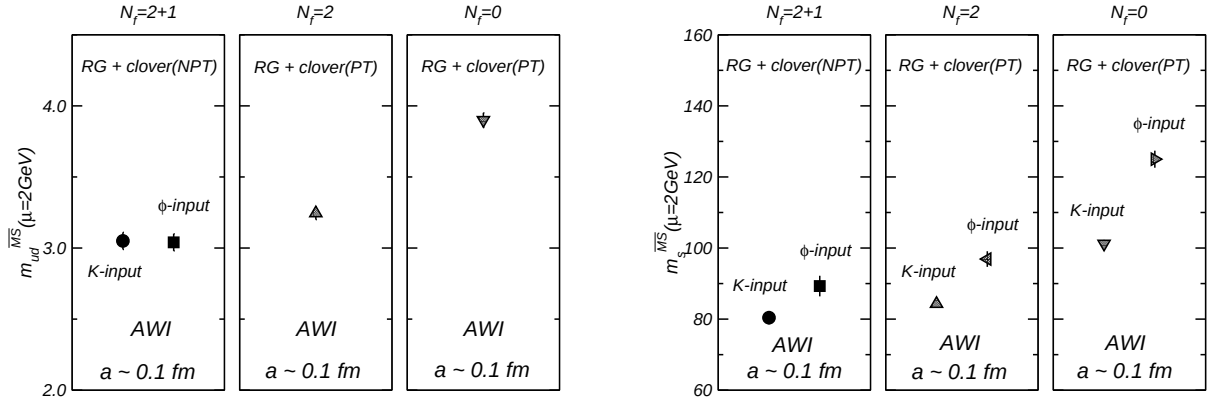

Figure 2. N_f dependence of light (left panel) and strange (right panel) quark masses at $a \sim 0.1$ fm from CP-PACS and JLQCD [17].

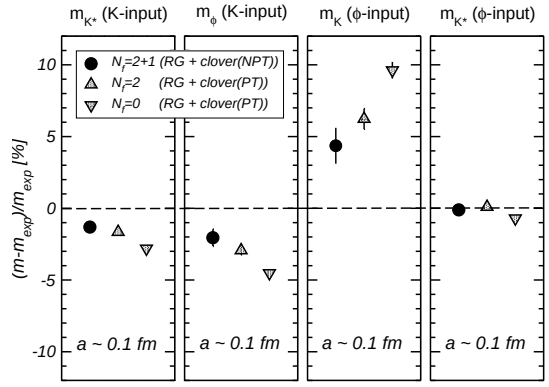

Figure 1. CP-PACS-JLQCD result for the N_f dependence of the light meson masses at $a \sim 0.1$ fm [17]. Circles represent the $N_f = 2 + 1$ result with RC(NP) [17], while triangles show the $N_f = 2$ and 0 data with RC(TP) [11].

by a simultaneous fit to LL, LS and SS masses with a polynomial fit function including up to quadratic terms of valence and sea quark masses.

Figure 1 shows the deviation of meson spectrum from the experiment value. Lattice data are shown for the 2+1 (filled circle), 2 (up triangle), and 0 (down triangle) dynamical flavors at $a \sim 0.1$ fm. The error bar shows statistical error only. Compared to the 2-flavor result, the 2+1-flavor simulation gives the result slightly closer to the experiment. Figure 2 shows the comparison of quark masses with different N_f at $a \sim 0.1$ fm. The reduction of quark mass with the inclusion of dynamical up and down quarks is significant. The effect of dynamical strange quark is, on the other hand, not conclusive at this stage, because there may be an effect of a different choice of $c_{\rm SW}$ yielding different scaling violation among the data. The light quark mass could be sensitive to the choice of the detail of the chiral extrapolation. The effect of the chiral logarithm should be investigated.

3.3. $N_f = 2+1$ simulation with the KS-type fermions

The MILC collaboration has been generating configurations of $N_f = 2+1$ QCD with the SZAT action. The HPQCD-MILC-UKQCD-Fermilab collaborations calculated the "gold-plated" observables on these configurations, and found results shown in Fig. 3. A good agreement is seen between the experimental and lattice results for $N_f = 3$ for a number of quantities covering both the light sector and the heavy sector.

This year the MILC collaboration published a detailed analysis of the continuum and chiral extrapolations [45,15]. Since the analysis of the light pseudo-scalar meson channel using ChPT is very important, and also instructive to the Wilson-type quark action simulations, I discuss the key points of their method to obtain the chiral and continuum limit in Sec. 4.

From this analysis, they obtain the light meson spectrum, the decay constants, and the low energy constants of chiral perturbation theory [45].

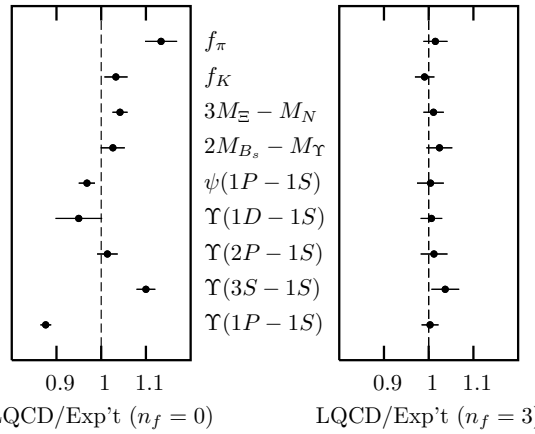

Figure 3. Lattice QCD results with SZAT action divided by experimental results for the "gold-plated" observables [30].

The light quark masses are also extracted [46]. The results for the pion and K meson decay constants are

$$\begin{aligned} f_\pi &= 129.5 \pm 0.9 \pm 3.5 \quad \text{MeV}, \\ f_K &= 156.6 \pm 1.0 \pm 3.6 \quad \text{MeV}, \\ f_K/f_\pi &= 1.210(4)(13), \end{aligned} \tag{1}$$

which are updated values of Fig. 3. The errors are statistical and systematic, the latter containing chiral and continuum extrapolations, the scale determination, and electromagnetic effects as carefully investigated in [15].

The strange quark mass m_s, and averaged up and down quark mass $\hat{m}$ in the $\overline{\rm MS}$ scheme at $O(\alpha_s)$ matching are given by

$$\begin{aligned} m_s^{\overline{\rm MS}} &= 76(0)(3)(7)(0) \quad \text{MeV}, \\ \hat{m}^{\overline{\rm MS}} &= 2.8(0)(1)(3)(0) \quad \text{MeV}, \\ m_s/\hat{m} &= 27.4(1)(4)(0)(1), \end{aligned} \tag{2}$$

where the errors are from statistics, simulations, perturbation theory and electromagnetic effects, respectively.

The light hadron spectrum reported in [15] is also an update of Fig. 3. The systematic errors from chiral extrapolation are not included in Fig. 16 of [15], but estimated in Fig. 4 of [15] for the nucleon mass.

An intersting work is discussion of the candidate of two-particle state for $0^{++}(a_0)$ and $1^{+-}(b_1)$ channel with the observation of the level crossing as decreasing the quark masses, although further clarification is still needed with smaller statistical error and smaller quark masses.

The heavy hadron mass splittings are obtained in [30], where the NRQCD action and Fermilab actions are used for b and c quarks respectively as shown in Fig. 3 (and also Fig. 16 of [15]).

A highlight of prediction from lattice QCD is the mass of B_c meson which is not well established experimentally. The current experimental value is 6.4(4) GeV from CDF [47] or 5.95(37) GeV from D0 preliminaly data [48]. Using the MILC configurations M_{B_c} has been calculated by the HPQCD-FNAL-UKQCD collaboration [49] applying the same technique to the heavy hadron spectrum described above. They obtained $M_{B_c} = 6.304(16)$ GeV. Comparions with future improved experiments will provide a verification of the technique used for the configuration generation.

4. Chiral extrapolation of hadronic observables

Consistency of lattice data with the chiral logarithm has been an important issue since the lattice 2002 conference [50]. Possible reasons for not finding the logarithm are : (1) quark masses are still too heavy to apply ChPT, and/or (2) lattice cutoff effect distorts the chiral logarithm. Both effects could be important for available simulation parameters [5]. Here we discuss recent results bearing on this question.

4.1. KS-type fermion action and SChPT

The MILC Collaboration use the staggered chiral perturbation theory (SChPT) as a guide in the chiral and continuum extrapolations [45,15]. SChPT represents the broken $SU(4 \times 3)_L \times SU(4 \times 3)_R$ symmetry, and incorporates both the taste symmetry breaking effect and fourth-root trick. The one-loop formula for the pseudoscalar masses and decay constants are obtained in [51,52,53]. Using the data at different lattice spacing and partially quenched [54] data sets, they simultaneously fit $M_{\rm PS}^2$ and $f_{\rm PS}$, and then the chiral and continuum limit can be taken at

the same time. They have two lattice spacings, $a \sim 0.125$ fm (coarse lattice) and ~ 0.09 fm (fine lattice). On the coarse lattice, five values of the light quark masses $a\hat{m}'$ corresponding to the range of $M_{\rm PS,LL}$ from 0.60 GeV to 0.25 GeV are simulated, and the strange quark mass am'_s is fixed at a slightly higher value than nature and the "K-meson" mass $M_{\rm PS,LS}$ ranges from 0.69 GeV to 0.58 GeV. On the fine lattice, two values of $a\hat{m}'$'s at a fixed am'_s are available to date, which correspond to $M_{\rm PS,LL} = 0.45$–0.32 GeV and $M_{\rm PS,LS} = 0.60$–0.55 GeV (the prime on mases means that they are the mass of dynamical quarks used in the simulations). In the fitting the partially quenched points are used, which could help to stabilize the fit [55]. In the MILC analysis the valence light quark masses are in the range $0.1m'_s$–m'_s.

The taste breaking effect appears in the mass splitting between Goldstone and non-Goldstone pions. With the AsqTad action the breaking of $O(\alpha^2 a^2)$ is expected, which is confirmed by measuring the ratio of the mass-squared splitting of fine to coarse lattice $(\Delta M^2)_{\rm fine}/(\Delta M^2)_{\rm coarse} \simeq (\alpha a^2)_{\rm fine}/(\alpha a^2)_{\rm coarse} = 0.372$. The splitting also shows the $SO(4)$ symmetry expected from SChPT [56].

The mass range where the (S)ChPT is valid is not known a priori. To see how large quark masses can be used in the chiral extrapolation they attempted the fit for different subsets of the data. The data subsets are:

- subset I (94 data points) with $m_x + m_y \leq 0.4m'_s$ (coarse) and $m_x + m_y \leq 0.54m'_s$ (fine).
- subset II (240 data points) with $m_x + m_y \leq 0.7m'_s$ (coarse) and $m_x + m_y \leq 0.8m'_s$ (fine).
- subset III (416 data points) with $m_x + m_y \leq 1.10m'_s$ (coarse) and $m_x + m_y \leq 1.14m'_s$ (fine),

where $m_{x(y)}$ means the mass of valence quark. They found that the NLO formula is not sufficient even if for the subset I (lightest set), for which the heaviest meson mass is around ~ 0.5 GeV. At this value the NNLO contribution is expected to be around $\sim 3.5\%$, which is larger than the statistical error (0.1%–0.7%). Since the full NNLO terms for SChPT is not known, they include analytic terms in the fitting ansatz. The NNNLO effect is also investigated. For future analysis full NNLO form for SChPT is desired.

The fit parameters include the effects of the scaling violation. Taste symmetry breaking terms could vary as $O(\alpha_s^2 a^2)$, and other parameters include dependence on $O(\alpha_s a^2)$ or $O(\alpha_s^2 a^2)$ in the global fitting. Thus, they investigated the following combination of fit ansatz and data sets to estimate various systematic errors.

- NNLO fit on subset I.
- NNLO fit on subset II.
- NNNLO fit on subset III.

where NNNLO fit is used to interpolate strange quark mass.

Figure 4 shows the result of simultaneous fitting (NNNLO fit on subset III). Selected data points and fit curves are presented. After the global fitting, the parameters are extrapolated to their continuum values, then the ChPT formula at continuum limit is recovered. The infinite volume limit is also taken.

Existence of the chiral logarithm could also be examined. Both the continuum logarithmic terms and taste breaking logarithms are needed to get good fits. Although the finite volume effect is expected to be small with their physical volume ($L > 2.5$ fm), it is observed that the fit degrades when the finite volume correction is switched off. The good fit is highly non-trivial and rely on the good statistics and partial quenching. It is not merely a consequence of the large number of fit parameters (40 parameters for NNLO fit).

The physical point is then derived by adjusting $\hat{m}'$ and m'_s with the ChPT formula at continuum limit to the corresponding mess masses and decay constants. They considered the electromagnetic and isospin violating effect when adjusting the physical point since their statistical precision are comparable to these effects. Thus the low energy constants, decay constants, quark masses are obtained [15,46].

They observed the chiral logarithm and obtained the best results in the chiral/continuum limit. For further improvement, study on scaling violation using three or more lattice spacing

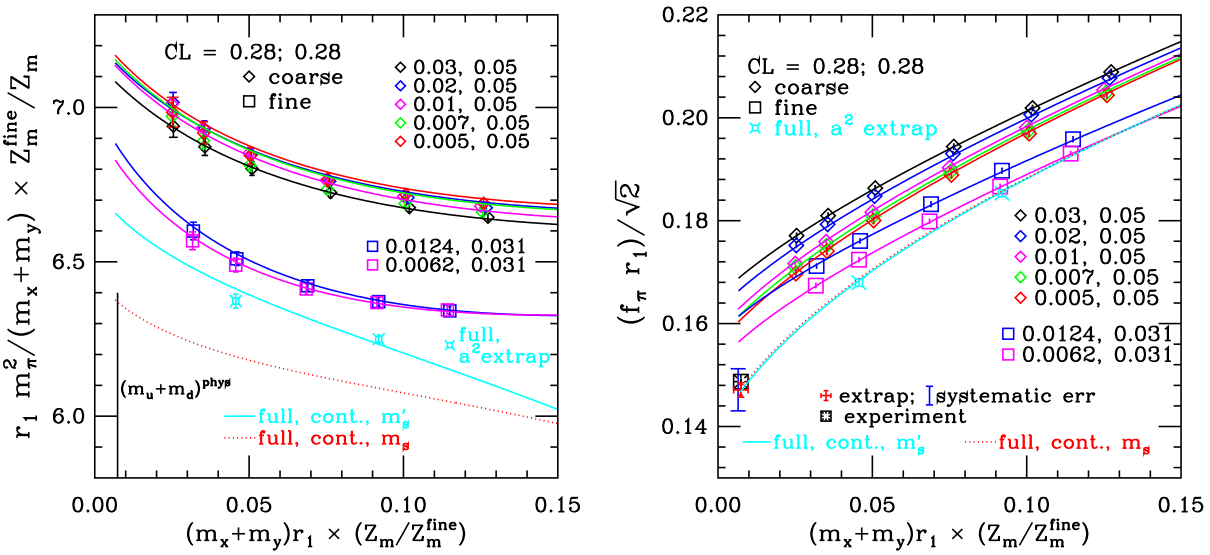

Figure 4. Global fit with partially quenched data sets from the MILC collaboration [45]. Valence quark mass dependence of $m_\pi^2/(m_x+m_y)$ (left panel) and $f_\pi/\sqrt{2}$ (right panel) in unit of r_1.

is desired, with which the assumptions on the scaling of the coefficients in the ChPT formula can be verified. The partially quenched NNLO formula is now available in the continuum theory [57], which would give hints to the NNLO SChPT calculations.

They observed that the ChPT formula gives a natural expansion with respect to the quark mass and taste symmetry breaking terms ($O(1)$ coefficients in the expansion). By a naive order counting NNLO contribution is $\sim 10\%$ even at $M_{\rm PS} \sim 600$ MeV. If we allow 10% statistical error, I think that NLO formula can only apply to the data set with $M_{\rm PS} \lesssim 600$ MeV, although MILC's analysis poses more tight restriction.

4.2. Wilson-type fermion action

The CP-PACS collaboration extended their coarse ($a = 0.22$ fm) lattice simulation [10] toward smaller quark mass region [18]. The simulation parameters are tabulated in Table 1. The lightest quark mass reaches $M_{\rm V}/M_{\rm PS} \sim 0.35$. They investigated the chiral behavior of pseudo-scalar meson mass, decay constant and PCAC quark mass.

The chiral fit is carried out with the continuum ChPT formula as well as the Wilson ChPT (WChPT) [58] formula, which contains the effect of scaling violation of $O(a)$ and $O(a^2)$. The former contribution can change the coefficient of the chiral logarithm; the latter introduces more singular logarithmic behavior and important to realize the Aoki phase [59]. Since the NLO calculation is not available for the partially quenched WChPT with the $O(a^2)$ effect, the fit is done on the unitary data set. Figure 5 shows the fits of the pseudo-scalar meson mass using the NLO ChPT with and without the scaling violation effects. The continuum NLO ChPT can fit data only below $M_{\rm PS} \simeq 630$ MeV (top panel), while the NLO WChPT can fit data up to $M_{\rm PS} \sim 1$ GeV.

The crucial test of the WChPT is to see whether it can explain the lattice spacing dependence of the data, which has been investigated using the $N_f = 2$ data from CP-PACS at four lattice spacings [58]. From the fits of available data at heavier mass region the scaling violation is not well described by the WChPT formula. They need simultaneous fit on PCAC quark masses, decay constants and meson masses, and smaller quark mass data including partially quenched data at finner lattice spacings in order

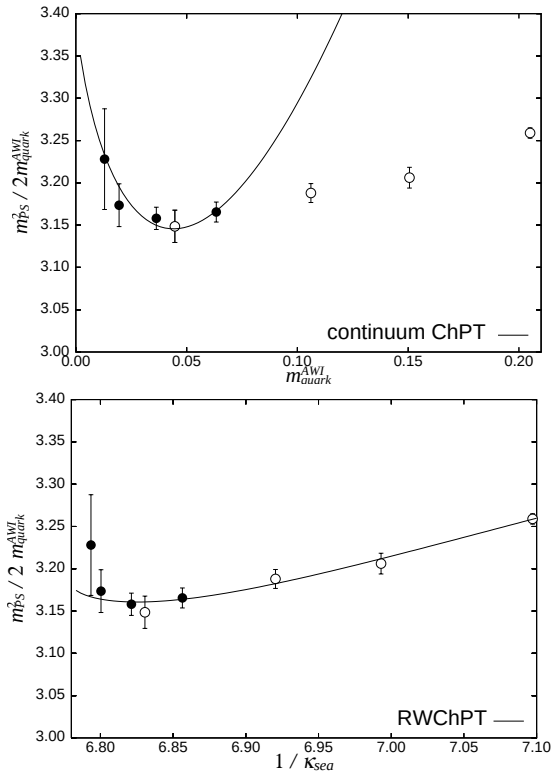

Figure 5. The continuum ChPT fit to the data $M_{\rm PS}/M_{\rm V} < 0.6$ (top panel), and the resummed Wilson ChPT fit to the whole data (bottom panel) [18].

to identify the $O(a)$ and $O(a^2)$ effects in the chiral fits.

The qq+q collaboration studied the chiral fit with the unimproved Wilson action [23,24] using the NLO WChPT formula including the $O(a)$ effects [60]. The simulation parameters are shown in Table 1, which cover the similar region as in [18]. They also estimate the (continuum) analytic NNLO contribution and the low energy constants of ChPT.

Using the double ratio method [4] they estimate the contribution of NNLO and $O(a)$ effect. Their data indicate that the $O(a)$ contribution is not important, but the NNLO is. It seems that this contradicts with the naive order counting for $a \sim 0.2$ fm (see also [5]). Because the qq+q data point $\beta = 5.1$ is close to the recently observed first order phase transition point $\beta = 5.2$ [61,62], and one may suspect that the data could be badly distorted. Therefore, one needs a detailed study of scaling to draw definite conclusion.

To further discuss this point, we show in Figure 6 the double ratio against the ratio of valence and sea quark masses $\xi = m_V/m_S$ from the partially quenched data at $a \sim 0.09$ fm of the JLQCD collaboration [20,63]. RRf and RRn are defined as

$$RRf = \frac{f_{VS}^2}{f_{SS} f_{VV}}, \tag{3}$$

$$RRn = \frac{4\xi}{(1+\xi)^2} \frac{M_{VS}^4}{M_{SS}^2 M_{VV}^2}, \tag{4}$$

with V denoting $m_{\rm val} \neq m_{\rm sea}$ and S means the unitary point [23]. The lines are the theoretically expected chiral logarithm at NLO in the continuum ChPT. Filled symbols ($M_S S \simeq$ 600 MeV) below $\xi = 1$ are close to the corresponding theoretical expectation, compared to the heavier quark mass data. It suggests that the ChPT is valid only below $M_{\rm PS} < 0.6$ GeV. The detailed scaling study and application of partially quenched WChPT formula including $O(a^2)$ effect is, however, needed again.

The UKQCD collaboration added a new data at $M_{\rm PS}/M_{\rm V} \sim 0.44$ ($M_{\rm PS} \sim 400$ MeV) [19] to the previous simulations [12]. Large finite volume effect is expected, since their physical volume is $L \sim 1.5$ fm and $M_{\rm PS} L = 3.2$ at the lightest data. They observed some curvature for the pseudo-scalar meson decay constant as a function of pseudo-scalar meson mass squared as shown in Figure 7. The bursts are the experimental values of f_π and f_K and the solid curve is the continuum ChPT curve fitted to the experimental values. The open boxes are the lattice data. The crosses are the decay constants in the finite volume ($L = 1.5$ fm) expected from continuum ChPT formula [64]. They argue that the curvature observed in lattice data is the result of finite volume effect from the chiral logarithm. Further clarification is, however, needed through the systematic study on the volume dependence and quark mass dependence.

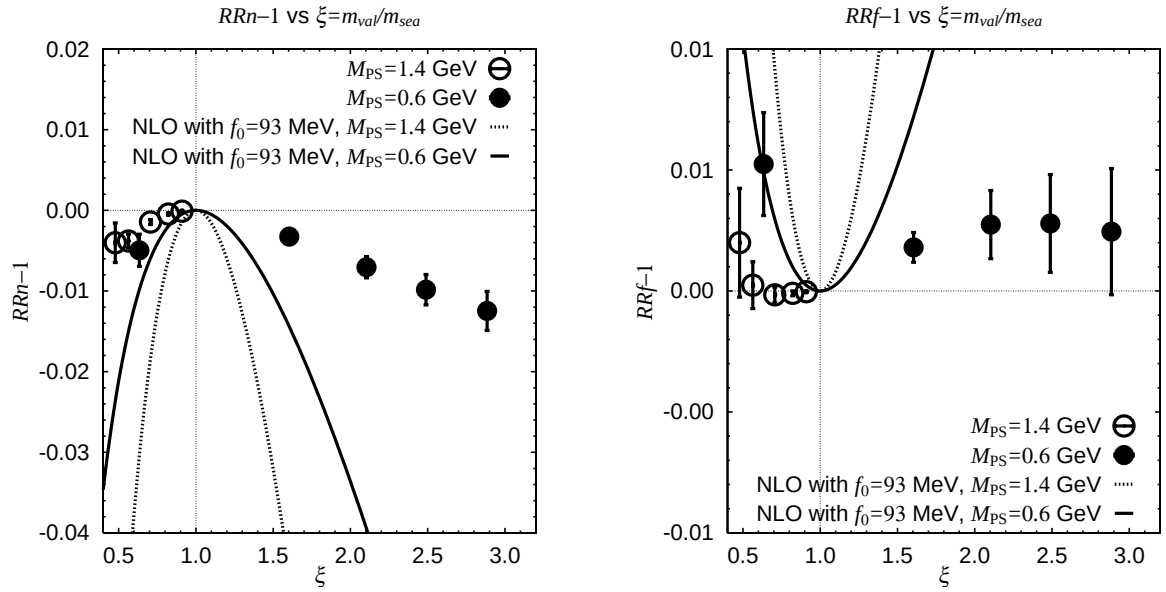

Figure 6. RRn and RRf as a function of ξ, data from JLQCD, $20^3 \times 48$, $M_{\rm PS}$ =0.6–1.4 GeV [20]

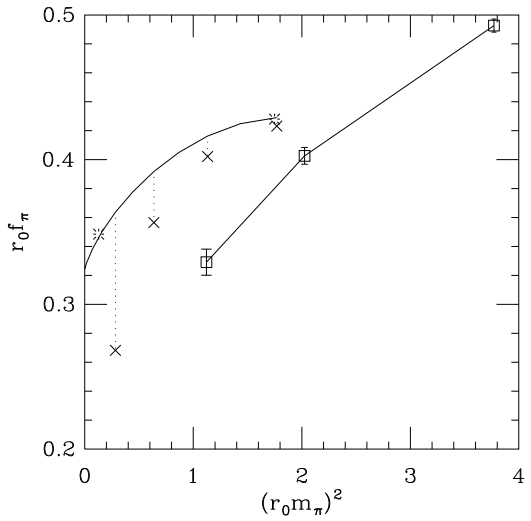

Figure 7. The pseudo-scalar decay constant as a function of the pseudo-scalar meson mass squared from UKQCD [19].

4.3. twisted mass QCD and a surprise of a first-order phase transition

Since the chirally twisted mass [65] introduces a lower bound on the eigenvalue of the (hermitian) Wilson-Dirac operator, the unquenched simulation could be substantially faster for small quark masses compared to the (untwisted) Wilson-type quarks. Two-flavor twisted mass Wilson quark simulations have been started and the first results are reported by [61]. Surprisingly, they found a strong metastability in the plaquette expectation value at $\beta = 5.2$ for twisted mass of $\mu = 0$–0.1. The quark mass determined through the PCAC relation changes its sign at the phase gap, and the pion mass does not vanish by tuning hopping parameter. The origin of the metastability may be attributed the possible scenario described in [59], that is that the negative coefficient of the $O(a^2)$ term in the chiral effective Lagrangian could cause the absence of the Aoki phase. This observation raises a new question on the phase structure in the (β, κ) plane in unquenched simulations with Wilson type quarks. To reach the chiral limit at finite lattice spacings one needs the Aoki phase separated by a second order phase transition, but it is not necessarily the case. Then, the chiral extrapolation must be done after taking the continuum limit. The extension of the phase diagram to twisted mass

direction is also investigated in the effective Lagrangian [66].

4.4. Domain-wall fermion

The RBC collaboration performed two-flavor dynamical simulations with the domain-wall quark action [31,22]. It is expected that the Ginsparg-Wilson (GW) type fermion has much better chiral property because of the exact chiral symmetry at finite lattice spacings. The domain wall fermion, however, in finite extent in the fifth dimension does not obey the GW relation exactly. The violation of the symmetry can be measured by the residual mass defined through the Ward-Takahashi identity of the DW fermion and the residual mass remains even in the massless limit. The lattice size in the fifth dimension is $N_s = 12$, with which the residual mass is small enough $am_{\rm res} \simeq 0.001$. Using three quark masses $m_{\rm sea} \sim m_s/2,\ 3m_s/4,\ m_s$, they analyzed the pseudo-scalar meson mass and the decay constant using continuum NLO ChPT formula. They observed that for the pseudo-scalar meson mass the partially quenched NLO ChPT can fit the data for $\leq 3m_s/4$ ($M_{\rm PS} \lesssim 630$ MeV), while χ^2 gets much worse if one includes the heavier mass data ($M_{\rm PS} \sim 690$ MeV). For the decay constant, the NLO formula cannot describe the data well even if one restrict the masses in $\leq 3m_s/4$ ($M_{\rm PS} \lesssim 630$ MeV). This is probably because of limited available data points compared to that of meson mass case. Although they observed $f_\pi/m_\rho = 0.170(8)$, and $f_K/m_\pi = 1.18(1)$ from the LO fit in fair agreement with experiment, the full NLO analysis with more data point would be needed to control the chiral extrapolation.

4.5. Summary

For the KS-type fermions the chiral logarithm is observed by the MILC collaboration for small sea quark masses using the SChPT formula. On the other hand, there is no definite conclusion for the Wilson-type fermions primarily because the unquenched simulations are still limited to relatively heavy quark masses. As a result, chiral extrapolation with appropriate ChPT formula in finite lattice spacing is not well investigated so far. Nevertheless, from the observation from the MILC results and the studies discussed in this section, it is likely that ChPT can only be applied at $M_{\rm PS} \lesssim 0.6$ GeV. For Wilson-type fermions, development of simulation algorithms that allow to enter this region [39] is crucial for progress.

5. Other topics on hadron spectrum

5.1. Mixed action simulations

The Ginsparg-Wilson fermions improve the chiral property. However, it is numerically so demanding that the unquenched simulations are hard task especially for light quarks. Use of different quark actions for valence and sea quarks can provide a clue to avoid too large computational cost while partly keeping the good chiral property. The partially quenched quark mass combinations can also be studied in this setup. A possible problem is the violation of unitarity, which can be removed only in the continuum limit.

As I already mentioned, the unquenched configurations with KS-type sea quarks reaches the chiral regime. Various measurements on these configurations have been carried out. The light hadron spectrum in Section 3.3 may also be considered as a mixed action calculation because the treatment of the KS-Dirac operator is different between valence and sea; while sea quarks are expressed by the fourth-root trick, valence quarks are treated by the quantum number projection.

Preliminary results for the light hadron spectrum with the overlap or domain wall valence quarks on the $N_f = 2 + 1$ KS-type sea quarks generated by the MILC collaboration have been reported in [67,68]. The valence mass is tuned by matching pseudo-scalar meson masses calculated with the domain wall and KS quarks [67].

5.2. Flavor singlet meson mass

The large splitting between the flavor singlet η' mass and other flavor octet meson masses should be explained by lattice QCD simulations. There have been a series of studies calculating the flavor singlet mass in unquenched simulations [69,70,71, 72,19,73].

The continuum limit of the η' mass in $N_f = 2$ was studied for the RC(T) action [71], and $M_{\eta'} = 960(87)(^{+\ 36}_{-248})$ MeV was obtained where the sys-

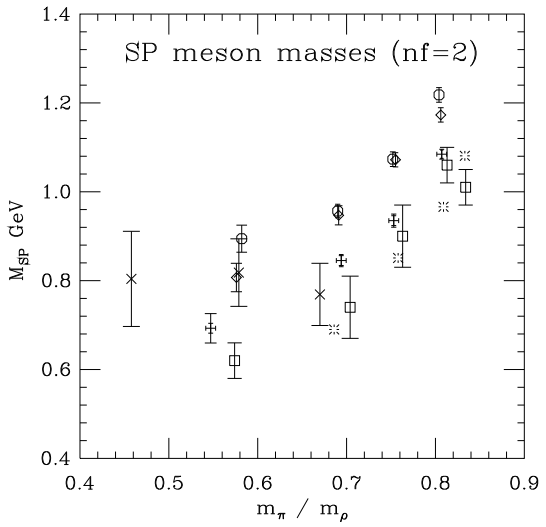

Figure 8. The η' meson mass in $N_f = 2$ as a function of $M_{\rm PS}/M_{\rm V}$ quoted from [19]. Results are obtained with PC [19,70] (crosses), PW [72] (bursts), PW [69] (squares), and RC(TP) [71] (diamond ($\beta = 2.1$), octagon ($\beta = 1.95$), fancy plus ($\beta = 1.8$)) actions.

tematic errors come from the continuum and chiral extrapolations. This value seems consistent with the experimental value $M_{\eta'} = 956$ MeV. However, the lattice result represents the value in the $N_f = 2$ world for which the expectation for the iso-singlet meson mass is 861 MeV (method described in [19,70]) or 715 MeV (from Witten-Veneziano formula). The above result from the RC(T) action is consistent within the error. The rather large systematic error in the negative direction comes from continuum extrapolation. It seems difficult to obtain a reliable continuum extrapolation because of large statistical errors even if we add some points with different lattice spacings around $a^{-1} = 2.5$ GeV. One would need a better method to improve the statistical signal. The chiral extrapolation should be carried out for both $M_{\rm PS}^2$ and $M_{\rm PS}$ as a linear function of $M_{\rm PS}^2$, since reliable fit ansatz is not known.

Figure 8 shows the $M_{\rm PS}/M_{\rm V}$ dependence of $M_{\eta'}$ compiled in [19]. The data show a similar dependence on $M_{\rm PS}/M_{\rm V}$ except for crosses. The data at lighter two crosses [19] ($a = 0.1$ fm) seems to be constant. Squares [69] are obtained with Z_2 noise method, while bursts [72,74] are obtained with truncated eigenvalue approximation (TEA) method from the same SESAM configuration [27] (symbols are slightly shifted horizontally to avoid overlapping). They are consistent with each other while the TEA has smaller statistical error. The value at physical point is different: $M_{\eta'} \sim 290$ MeV with TEA [72,74] and $\sim 520^{+125}_{-58}$ MeV with Z_2 [69]. Systematic study of chiral extrapolation with more data at smaller quark masses will clarify the difference of these data. The 10–20% scaling violantion from $O(a\Lambda_{\rm QCD})$ error is also expected with unimproved gauge and quark actions even at $a^{-1} \sim 2.3$ GeV lattice.

The effect of η and η' mixing can be treated by the partially quenched strange analysis within the $N_f = 2$ simulations [72,74,70,73]. The quadratic mass matrix in the quark-flavor basis is obtained in [72,74,70] on the $a^{-1} \sim 2.3$ GeV SESAM configurations and they obtained $M_\eta = 292(31)$ MeV and $M_{\eta'} = 686(31)$ MeV after the diagonarilzation of the mass matrix. While these individual numbers are still below the experimental numbers, the splitting is comparable to the experimental value.

5.3. Universality of quenched hadron spectrum

Sometime ago, it was pointed out that the values of $M_{\rm N}/M_{\rm V}$ at $M_{\rm PS}/M_{\rm V} = 0.5$ disagree in the continuum limit between the PKS action and PW (RC(TP)) action [75]. The PKS data in $aM_{\rm V} < 1.4$ were extrapolated with a function $c_0 + c_1 \times a^2$, and the PW (RC(TP)) data in $aM_{\rm V} < 1$ were extrapolated with $c_0 + c_1 \times a$.

This year reanalysis is done by adding new data with various lattice actions generated since 2000 [76]. The universality is investigated in the quenched approximation by checking the consistency in the continuum limit among the various discretization method using the Bayesian fitting approach [77]. All the data are simultaneously fitted with some constraints. The fit functions are polynomials which contains leading and higher order terms as a function of $aM_{\rm V}$ (for the KS-type action only a^{2n} terms are included) with a common continuum limit. The coefficients are constrained to stay within reasonable values by the

Bayesian prior. Thus, they obtained a reasonable χ^2 value for the consistent continuum limit. The continuum value is 2σ below and 4σ below from the previous analysis of the PK and PW actions respectively. They also investigated the universal continuum limit of $M_{\rm V}r_1$ and $M_{\rm N}r_1$ with more data (lattice actions) and obtained a reasonable χ^2 values. These tests suggest the difficulty to estimate the systematic error of continuum extrapolation from single lattice action and the importance of the action improvement with many lattice spacings. The similar test for universality should eventually be done for unquenched simulations.

6. Conclusions

The unquenched QCD simulations with dynamical up, down and strange quarks have made significant development over the past year. The progress has been more notable for the KS-type fermions for which an extensive work has been made both in pushing the simulations toward small quark masses and in analyzing the results. Applying staggered ChPT, it was shown that their data are consistent with the expected logarithmic chiral behavior once the pseudo scalar meson masses are decreased below $M_{\rm PS} < 0.6$ GeV. Worries, however, regarding the field theoretic foundation of the fourth-root trick mandatory in $N_f = 2 + 1$ simulations with the KS-type fermions still need to be clarified.

Simulations with the Wilson-type fermions yielded an encouraging result that the meson spectrum moves progressively close to experiment as the number of dynamical quarks increases from $N_f = 0$ to 2 to $2+1$. The largest issue is the long chiral extrapolation from heavy quark masses involved in reaching this result; consistency with the expected chiral behavior is not established to satisfaction. Hence algorithms which allow simulations with quark masses as light as used in the KS-type fermions are deeply needed. As we encountered for nucleon mass in the quenched case, cross checks between the KS-type and Wilson-type fermions which will be made possible by such algorithms are very important for establishing unquenched predictions.

Looking further ahead, unquenched simulations with the Ginsparg-Wilson type quark actions with the correct chiral behavior are the most challenging issue in future lattice QCD.

I would like to thank all the colleagues who made their results available before the conference. I also thank S. Hashimoto and A Ukawa for valuable comments and proof reading on the manuscript. This work is supported in part by the Grants-in-Aid of Ministry of Education (Nos. 16740147, 15204015).

REFERENCES

1. S. Duane, A. D. Kennedy, B. J. Pendleton and D. Roweth, Phys. Lett. B **195** (1987) 216.
2. S. A. Gottlieb, W. Liu, D. Toussaint, R. L. Renken and R. L. Sugar, Phys. Rev. D **35** (1987) 2531.
3. T. Takaishi and P. de Forcrand, Int. J. Mod. Phys. C **13** (2002) 343 [arXiv:hep-lat/0108012]; T. Takaishi and P. de Forcrand, Nucl. Phys. Proc. Suppl. **94** (2001) 818 [arXiv:hep-lat/0011003].
4. S. Hashimoto *et al.* [JLQCD Collaboration], Nucl. Phys. Proc. Suppl. **119** (2003) 332 [arXiv:hep-lat/0209091].
5. O. Bär, "Chiral Perturbation Theory at Non-Zero a", contribution to this conference.
6. G. Colangelo, "Chiral Perturbation Theory in Finite Volume", contribution to this conference.
7. V. Lubicz, "Lattice QCD and Flavor Physics", contribution to this conference.
8. M. Wingate, "Status of Lattice Flavor Physics", contribution to this conference.
9. P. Rakow, "QCD Coupling and Quark Masses", contribution to this conference.
10. A. Ali Khan *et al.* [CP-PACS Collaboration], Phys. Rev. Lett. **85** (2000) 4674 [Erratum-ibid. **90** (2003) 029902] [arXiv:hep-lat/0004010];
11. A. Ali Khan *et al.* [CP-PACS Collaboration], Phys. Rev. D **65** (2002) 054505 [Erratum-ibid. D **67** (2003) 059901] [arXiv:hep-lat/0105015].
12. C. R. Allton *et al.* [UKQCD Collaboration], Phys. Rev. D **60** (1999) 034507

[arXiv:hep-lat/9808016]; C. R. Allton *et al.* [UKQCD Collaboration], Phys. Rev. D **65** (2002) 054502 [arXiv:hep-lat/0107021].
13. C. W. Bernard *et al.*, Phys. Rev. D **62** (2000) 034503 [arXiv:hep-lat/0002028]; C. W. Bernard *et al.*, Phys. Rev. D **64** (2001) 054506 [arXiv:hep-lat/0104002].
14. S. A. Gottlieb, Nucl. Phys. Proc. Suppl. **128** (2004) 72 [Nucl. Phys. Proc. Suppl. **129** (2004) 17] [arXiv:hep-lat/0310041].
15. C. Aubin *et al.*, arXiv:hep-lat/0402030.
16. T. Kaneko *et al.* [CP-PACS and JLQCD Collaborations], Nucl. Phys. Proc. Suppl. **129** (2004) 188 [arXiv:hep-lat/0309137].
17. T. Ishikawa *et al.* [CP-PACS and JLQCD Collaborations], contribution to this conference.
18. Y. Namekawa *et al.* [CP-PACS Collaboration], arXiv:hep-lat/0404014; Y. Namekawa, contribution to this conference.
19. C. R. Allton *et al.* [UKQCD Collaboration], Phys. Rev. D **70** (2004) 014501 [arXiv:hep-lat/0403007]; C. McNeile, contribution to this conference.
20. S. Aoki *et al.* [JLQCD Collaboration], Phys. Rev. D **68** (2003) 054502 [arXiv:hep-lat/0212039].
21. A. Ali Khan *et al.* [QCDSF-UKQCD Collaboration], Nucl. Phys. B **689** (2004) 175 [arXiv:hep-lat/0312030]; A. Ali Khan *et al.* [QCDSF Collaborations], arXiv:hep-lat/0312029; A. Ali Khan *et al.* [QCDSF Collaboration], Nucl. Phys. Proc. Suppl. **129** (2004) 176 [arXiv:hep-lat/0309133].
22. C. Dawson, T Izubuchi [RBC Collaboration], contributions to this conference.
23. F. Farchioni, I. Montvay, E. Scholz and L. Scorzato [qq+q Collaboration], Eur. Phys. J. C **31** (2003) 227 [arXiv:hep-lat/0307002]; F. Farchioni, C. Gebert, I. Montvay, E. Scholz and L. Scorzato [qq+q Collaboration], Nucl. Phys. Proc. Suppl. **129** (2004) 179 [arXiv:hep-lat/0309094].
24. F. Farchioni, I. Montvay and E. Scholz [qq+q Collaboration], arXiv:hep-lat/0403014; F. Farchioni, I. Montvay and E. Scholz [qq+q Collaboration], arXiv:hep-lat/0409004, contribution to this conference.
25. D. Becirevic *et al.* [SPQcdR Collaboration], contribution to this conference.
26. B. Orth, T. Lippert and K. Schilling, Nucl. Phys. Proc. Suppl. **129** (2004) 173 [arXiv:hep-lat/0309085].
27. N. Eicker *et al.* [TXL collaboration], Phys. Rev. D **59** (1999) 014509 [arXiv:hep-lat/9806027].
28. T. Lippert *et al.*, Nucl. Phys. Proc. Suppl. **60A** (1998) 311 [arXiv:hep-lat/9707004].
29. N. Eicker, T. Lippert, B. Orth and K. Schilling, Nucl. Phys. Proc. Suppl. **106** (2002) 209 [arXiv:hep-lat/0110134].
30. C. T. H. Davies *et al.* [HPQCD Collaboration], Phys. Rev. Lett. **92** (2004) 022001 [arXiv:hep-lat/0304004].
31. T. Izubuchi [RBC Collaboration], Nucl. Phys. Proc. Suppl. **129** (2004) 266 [arXiv:hep-lat/0310058]; T. Izubuchi [RBC Collaboration], Nucl. Phys. Proc. Suppl. **119** (2003) 813 [arXiv:hep-lat/0210011].
32. D. H. Weingarten and D. N. Petcher, Phys. Lett. B **99**, 333 (1981).
33. Another factorization method for single flavor simulations, see : T. Lippert, Lect. Notes Comput. Sci. **15** (2000) 166 [arXiv:hep-lat/0007029].
34. S. Aoki *et al.* [JLQCD Collaboration], Phys. Rev. D **65** (2002) 094507 [arXiv:hep-lat/0112051].
35. M. A. Clark, B. Joo and A. D. Kennedy, Nucl. Phys. Proc. Suppl. **119** (2003) 1015 [arXiv:hep-lat/0209035];
36. M. A. Clark and A. D. Kennedy, Nucl. Phys. Proc. Suppl. **129** (2004) 850 [arXiv:hep-lat/0309084];
37. A. D. Kennedy, I. Horvath and S. Sint, Nucl. Phys. Proc. Suppl. **73** (1999) 834 [arXiv:hep-lat/9809092].
38. S. Aoki *et al.* [JLQCD Collaboration], Comput. Phys. Commun. **155** (2003) 183 [arXiv:hep-lat/0208058].
39. A. D. Kennedy, "Algorithms for Lattice QCD", contribution to this conference.
40. B. Bunk, M. Della Morte, K. Jansen and F. Knechtli, Nucl. Phys. B **697** (2004) 343 [arXiv:hep-lat/0403022]; B. Bunk, M. Della Morte, K. Jansen and F. Knechtli,

arXiv:hep-lat/0408048, contribution to this conference.
41. A. Hart and E. Muller, arXiv:hep-lat/0406030.
42. K. Jansen, Nucl. Phys. Proc. Suppl. **129** (2004) 3.
43. D. Adams, "Universality of Lattice QCD", contribution to this conference.
44. E. Follana, "Index Theorem with Improved Staggered Quarks", contribution to this conference.
45. C. Aubin *et al.* [MILC Collaboration], arXiv:hep-lat/0407028; C. Bernard, contribution to this conference.
46. C. Aubin *et al.* [HPQCD Collaboration], Phys. Rev. D **70** (2004) 031504 [arXiv:hep-lat/0405022].
47. CDF, F. Abe *et al.*, Phys. Rev. Lett. **81** (1998) 2432.
48. R. Jesik, B physics at DØ, Unpublished talk given at Imperial College London, 2004.
49. I. F. Allison *et al.*, arXive:hep-lat/0409090, contribution to this conference.
50. C. Bernard, S. Hashimoto, D. B. Leinweber, P. Lepage, E. Pallante, S. R. Sharpe and H. Wittig, Nucl. Phys. Proc. Suppl. **119** (2003) 170 [arXiv:hep-lat/0209086].
51. C. Aubin and C. Bernard, Phys. Rev. D **68** (2003) 034014 [arXiv:hep-lat/0304014].
52. C. Aubin and C. Bernard, Phys. Rev. D **68** (2003) 074011 [arXiv:hep-lat/0306026].
53. C. Aubin and C. Bernard, Nucl. Phys. Proc. Suppl. **129** (2004) 182 [arXiv:hep-lat/0308036].
54. C. W. Bernard and M. F. L. Golterman, Phys. Rev. D **49** (1994) 486 [arXiv:hep-lat/9306005].
55. S. R. Sharpe and N. Shoresh, Phys. Rev. D **62** (2000) 094503 [arXiv:hep-lat/0006017].
56. W. Lee and S. R. Sharpe, Phys. Rev.**D** 60 (1999) 114503.
57. J. Bijnens, N. Danielsson, T. A. Lahde, hep-lat/0406017.
58. S. Aoki, Phys. Rev. D **68** (2003) 054508 [arXiv:hep-lat/0306027].
59. S. R. Sharpe and R. J. Singleton, Phys. Rev. D **58** (1998) 074501 [arXiv:hep-lat/9804028].
60. G. Rupak and N. Shoresh, Phys. Rev. D **66** (2002) 054503 [arXiv:hep-lat/0201019].
61. F. Farchioni *et al.*, arXiv:hep-lat/0409098, contribution to this conference.
62. F. Farchioni *et al.*, arXiv:hep-lat/0406039.
63. S. Hashimoto (JLQCD collaboration), private communication.
64. G. Colangelo and S. Durr, Eur. Phys. J. C **33** (2004) 543 [arXiv:hep-lat/0311023]; G. Colangelo and C. Haefeli, Phys. Lett. B **590** (2004) 258 [arXiv:hep-lat/0403025].
65. R. Frezzotti, "Twisted mass Lattice QCD", contribution to this conference.
66. S. R. Sharpe and J. M. S. Wu, arXiv:hep-lat/0407025; S. R. Sharpe and J. M. S. Wu, contribution to this conference.
67. W. Schroers, contribution to this conference.
68. R. J. Tweedie, contribution to this conference.
69. T. Struckmann *et al.* [TXL Collaboration], Phys. Rev. D **63** (2001) 074503 [arXiv:hep-lat/0010005]; T. Struckmann *et al.* [TXL collaboration], arXiv:hep-lat/0006012.
70. C. McNeile and C. Michael [UKQCD Collaboration], Phys. Lett. B **491** (2000) 123 [Erratum-ibid. B **551** (2003) 391] [arXiv:hep-lat/0006020].
71. V. I. Lesk *et al.* [CP-PACS Collaboration], Phys. Rev. D **67** (2003) 074503 [arXiv:hep-lat/0211040].
72. K. Schilling, H. Neff and T. Lippert, arXiv:hep-lat/0401005.
73. L. Venkataraman and G. Kilcup, arXiv:hep-lat/9711006.
74. H. Neff, T. Lippert, J. Negele and K. Schilling, Nucl. Phys. Proc. Suppl. **129** (2004) 218 [arXiv:hep-lat/0401004]; H. Neff, T. Lippert, J. W. Negele and K. Schilling, Nucl. Phys. Proc. Suppl. **119** (2003) 251 [arXiv:hep-lat/0209117].
75. S. Aoki, Nucl. Phys. Proc. Suppl. **94** (2001) 3 [arXiv:hep-lat/0011074].
76. C. T. H. Davies, G. P. Lepage, F. Niedermayer and D. Toussaint, arXiv:hep-lat/0409039, contribution to this conference.
77. G. P. Lepage, B. Clark, C. T. H. Davies, K. Hornbostel, P. B. Mackenzie,

C. Morningstar and H. Trottier, Nucl. Phys. Proc. Suppl. **106** (2002) 12 [arXiv:hep-lat/0110175].